J Therm Anal Calorim (2010) 100:361–366
DOI 10.1007/s10973-009-0587-1

DSC analysis of Al6061 aluminum alloy powder by rapid solidification

Effect of additives

Antonyraj Arockiasamy · Randall M. German · Paul Wang · Mark F. Horstemeyer · Pavan Suri · S. J. Park

Received: 19 March 2009 / Accepted: 26 October 2009 / Published online: 11 December 2009

Abstract Differential scanning calorimetry (DSC) is a powerful technique that measures the heat evolution from a sample under a controlled condition and studies the phase transformation, precipitation, and dissolution activities. In this work, we investigated the influence of admixed silicon and silicon carbide and the effect of different atmospheres on the heat flow properties and microstructure of atomized Al6061 powder using DSC and scanning electron microscopy. The DSC analysis revealed the addition of silicon considerably decreased the temperature of first endothermic peaks. With an increase in silicon content the enthalpy for the first endothermic peak increased, whereas the second endothermic peak decreased. An endothermic peak, indicating the formation of AlN, was observed for powders without the silicon addition, but was noticeably absent in the case of alloys with Si addition. The SiC addition has no influence on changing the enthalpy of the systems we investigated. The reason for this behavior is analyzed and presented in this article.

Keywords Al6061 powder · Alloying elements · Composites · Differential scanning calorimeter

A. Arockiasamy (✉) · P. Wang · M. F. Horstemeyer · S. J. Park
Center for Advanced Vehicular Systems, Mississippi State University, 200 Research Boulevard, Starkville, MS 39759, USA
e-mail: aanton@cavs.msstate.edu

R. M. German
College of Engineering, San Diego State University, 5500 Campanile Drive, San Diego, CA 92182-1326, USA

P. Suri
Heraeus, 301 N Roosevelt Ave, Chandler, AZ 85226, USA

Introduction

One of the primary aims for research related to materials for automotive and aeronautic applications is to reduce the weight of the components while improving the mechanical properties to boost fuel economy. This generates greater need for materials that exhibit high strength and stiffness. Metal matrix composites (MMC) provide a recognized opportunity to meet this performance combination [1]. Additions of reinforcements such as Al_2O_3, B_4C, or SiC are found to change the mechanical properties with an increased strength, elastic modulus, wear resistance, and high fatigue cycle relative to unreinforced aluminum. Automotive and aerospace industries utilize the excellent performance of these composites for various applications [2–4]. Still, manufacturers encounter some difficulties with this. One difficulty is the machinability of these materials due to the highly abrasive and intermittent nature of the reinforcements. Another factor is the high processing cost of these materials. The commonly available manufacturing processes are forging, rolling, and extrusion or near-net shape processing by casting or powder metallurgy. Among them, near-net shape processing by employing powder metallurgical route is the most cost efficient. Several aluminum alloy compositions are currently being developed [5]. The common Al6061 alloy is a suitable matrix for improved mechanical strength with Si and SiC as the principal alloying elements. Some articles reported the formation of Al_4C_3 as an intermediate product during melting Al with reinforced particles containing Si [6–8]. However, the addition of 20 vol% SiC particles increases the strength of Al6061 alloy [9, 10]. Silicon addition reduced the process temperature because of low melting phases and phase transformations. Due to the limited knowledge of the interfacial reaction between the reinforcement and the matrix during melting, the selection of

this composite is valuable for the development of this kind of advanced materials [11–13]. In this investigation, differential scanning calorimetry (DSC) was used to study the effect of various amounts of Si and SiC on changing the melting, dissolution, and precipitation behavior of a rapidly atomized Al6061 alloy. Scanning electron microscopy and energy dispersive spectroscopy were also used to identify the secondary phases present within the microstructure.

Experimental

Materials

Materials used in this study are argon atomized Al6061 (Epson ATMIX Corporation, Japan) with 99.5% purity and the particle size between 75 and 150 μm, Si (CERAC, Inc., USA) with 99.5% purity and particle size between 45 and 75 μm, and SiC (CERAC, Inc., USA) with 99.6% purity and particle size between 45 and 75 μm. The chemical composition of the atomized powder is given in Table 1, and characteristic features of the powder mixtures are provided in Table 2. As shown in Fig. 1, the shape and morphology of the Al, Si, and SiC powders, examined by scanning electron microscope (SEM), are round ligament shape, irregular shape, and pyramidal shape, respectively.

Mixing

Alloy mixtures were prepared by combining different powders as detailed in Table 3. These powder mixtures were blended for 20 min to give a homogeneous distribution. Physical properties such as apparent density ρ_a, tap density ρ_{tap}, pycnometer density ρ_{th}, and powder flow rate were measured according to ASTM standards and the values are given in Table 2.

DSC experiment

The DSC experiments were conducted using a SetSys Setaram Instrumentation Technologies, Inc., in the temperature range of 298–973 °K at a constant heating and cooling rate of 5 °C/min. An alumina crucible with a capacity of 75 μL was used. Baseline correction was performed in two stages. First, the DSC run with an empty crucible was subtracted from the experiment. Second, the data were corrected by assuming the combined effect of heat capacity differences and baseline fluctuations results in a heat flow, which is a second order polynomial.

Table 1 Chemical compositions of Al6061 alloy

Element	Al	Mg	Si	Cu	Fe	Cr	Zn	Mn	Ti
wt%	Balanced	0.90	0.65	0.32	0.20	0.07	0.03	0.02	0.02

Table 2 Powder characterization

Material	Al6061	Si	SiC
Particle size/μm	150	−325 mesh (−45 μm)	−325 mesh (−45 μm)
Apparent density/g cm^{-3}	0.73	0.70 (29.7%)	1.32 (40.4%)
Tap density/g cm^{-3}	1.18	0.96 (40.7%)	1.61 (49.2%)
Pycnometer density/g cm^{-3}	2.64	2.36	3.27

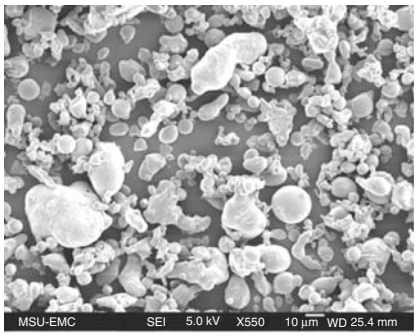

(a)

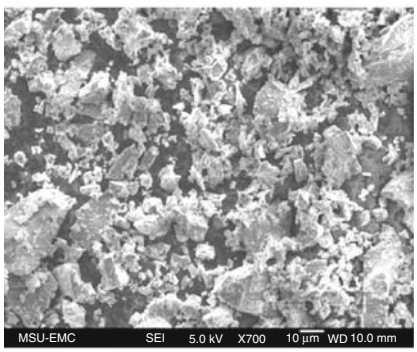

(b)

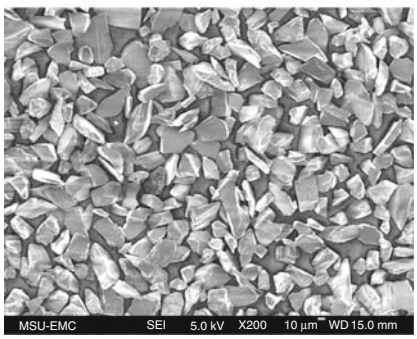

(c)

Fig. 1 Scanning electron micrographs of powders **a** Al6061, **b** Si, and **c** SiC

Table 3 Compositions of the alloys studied

Alloy ID	Si/wt%	SiC/wt%	Al6061
1	0.0	0.0	Balanced
2	2.5	0.0	
3	5.0	0.0	
4	10.0	0.0	
5	0.0	10.0	
6	10.0	10.0	

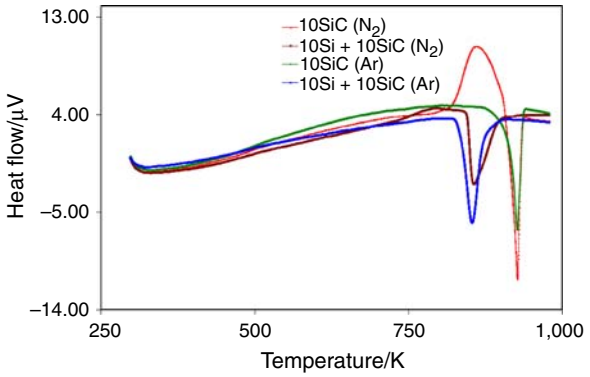

Fig. 2 DSC curves for alloy mixtures in both N_2 and Ar atmosphere

Metallography

Microstructural examination was carried out using a JEOL JSM-6500F scanning electron microscope (SEM) for the powders. Energy dispersive X-ray spectroscopy (EDS) attached to SEM analyzed the phases present within the microstructure of the sample that was tested in DSC.

Results and discussion

Effect of nitrogen atmosphere

Atmosphere plays a vital role in determining the mechanical properties of the parts. Dry nitrogen is the most common atmosphere used [14–18]. A vacuum is more effective than argon and hydrogen, which are detrimental to sintered density due to reduction of oxide and generation of water vapor at high temperatures resulting in pore generation and coarsening [14, 16].

The DSC curves for the investigated alloys in nitrogen (dew point: −55 °C) and argon are presented in Fig. 2. These results show that the endothermic peaks originated in the range of 873–938 °K in nitrogen and argon atmospheres is due to melting of Al6061. However, in nitrogen there is an additional exothermic peak at 866 °K with a reaction enthalpy of 61 mV s/mg in the alloy containing only SiC.

Samples collected after the DSC run were analyzed by SEM–EDS, which is shown in Fig. 3. EDS analysis was performed in two different locations and the composition of the phases present revealed the presence of AlN (Fig. 3a, b, Table 4). From these results, it is inferred that the exothermic peak corresponds to the reaction between aluminum and nitrogen to form AlN. There are reports [9, 10] which reveal the existence of AlN in the sintered aluminum alloy containing Mg when sintered in nitrogen. The formation of AlN may possibly reduce the pressure in the pore spaces relative to the external atmosphere, which induces pore filling by liquid or gas reaction products. As such, pore filling is an important densification mechanism during sintering. Formation of AlN disrupts the surface aluminum oxide to facilitate the diffusion processes [1, 4, 16]. Further, the resulting AlN dispersions increase the mechanical properties such as hardness, tensile strength, and wear resistance.

In the case of mixture containing both Si and SiC (10 wt% each) heated in N_2 the onset temperature decreased to 819 °K, and the matrix alloy completely melted at 853 °K (melting of matrix alloy reached at its maximum) with reaction enthalpy of 72 mV s/mg. In Ar the alloy showed the onset temperature of 834 °K, and the matrix alloy completely melted at 853 °K (melting of matrix alloy reached at its maximum) with the same reaction enthalpy of 72 mV s/mg. The change in onset temperature indicates the change in driving force for the alloy melting. The alloy melt at low temperature in N_2 atmosphere.

Effect of silicon content

The effect of Si on DSC thermograms is shown in Fig. 4. The endothermic peaks observed in a DSC scan of Al6061 with 2.5–10 wt% Si alloy in the temperature range 823–848 °K are due to the reaction of aluminum with silicon near the eutectic temperature. On continued heating, second

Table 4 EDS results for the Al6061 alloys in N_2

Spectrum	Al/wt%	Mg/wt%	Si/wt%	N/wt%	O/wt%	C/wt%	Fe/wt%
Spectrum 1	66.3	6.4	0.5	9.2	16.4	0.0	1.1
Spectrum 2	20.9	1.3	0.2	16.9	13.9	46.8	0.0

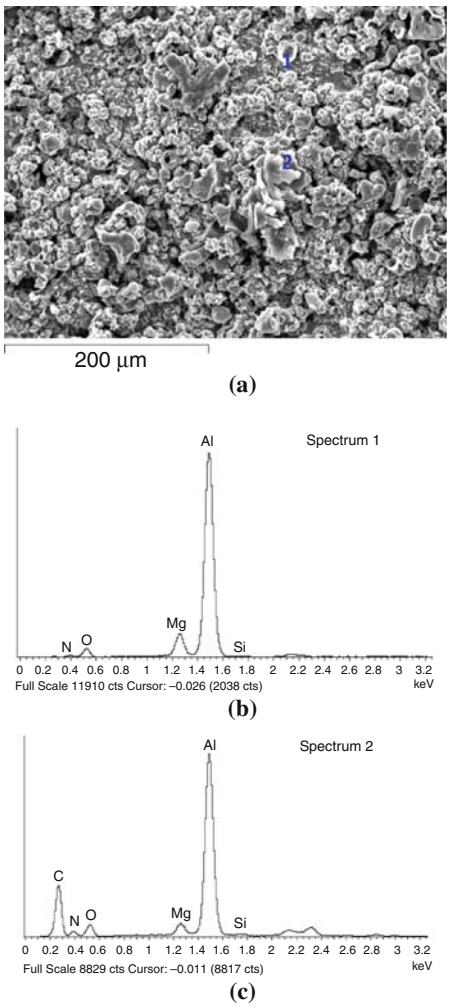

Fig. 3 SEM–EDS analysis for Al6061 in N_2 atmosphere. **a** SEM image. **b** EDS analysis at location 1 in the SEM image. **c** EDS analysis at location 2 in the SEM image

endothermic peaks appeared in the temperature range of 853–923 °K. This is ascribed to the dissolution of aluminum and Al–Si particles. Aluminum and silicon reacting in the Al-rich phase depends on the gross silicon content of the alloy.

Figure 5 shows Al–Si phase diagram which shows a maximum solubility at a silicon content of 13 at.% [19]. On heating, silicon, which was initially dissolved in the Al-rich matrix, precipitates and forms two phases, namely an Al-rich phase (matrix) and a Si rich phase (finely dispersed particles). It is well known that the melting point of pure aluminum is 933 °K, while the eutectic temperature is 850 °K in binary Al–Si system.

On comparison of these curves, the shape and temperature range of the endothermic peak significantly depends on the silicon content. The endothermic peak height for the alloy containing 10Si alloy is larger than the alloy containing a lesser amount of Si. Therefore, the heat effect for the former case is much larger than that of the latter

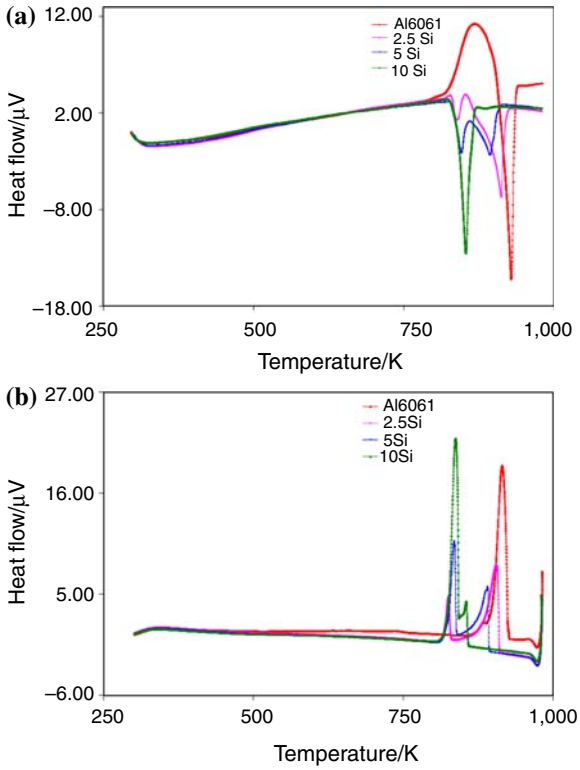

Fig. 4 DSC curves for Al6061 containing various amounts of Si **a** heating and **b** cooling cycle

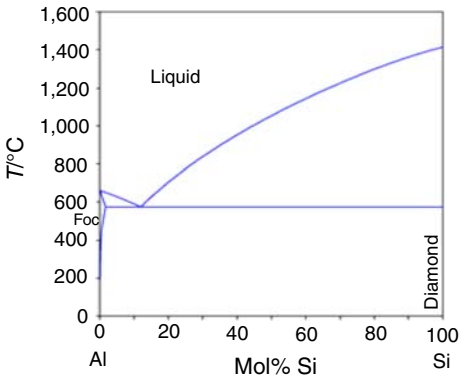

Fig. 5 Al–Si phase diagrams [19]

because the driving force for dissolution is larger for Al–10Si alloy due to the larger supersaturation. The heat production starts at a lower temperature in the DSC scan.

After the heating scan was completed ($T = 973$ °K), the system was slowly cooled to room temperature (Fig. 4b) at a controlled heating rate of 5 °C/min and aluminum (temperature range 928–888 °K) and Al–Si (848–803 °K) precipitates. In the case of high content of silicon, the second endothermic peak immediately following and overlapping with the first exothermic peak, a precipitation effect was observed. This effect is attributed to coarsening of the Al–Si particles.

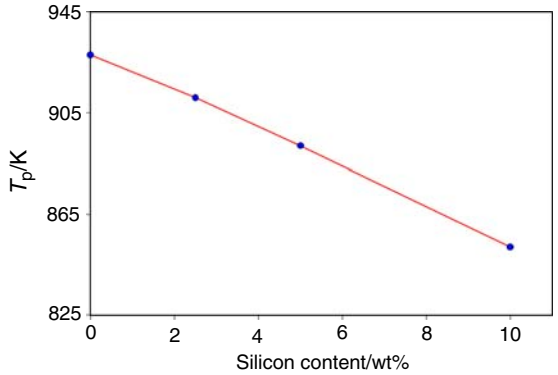

Fig. 6 Peak temperature of the endothermic peak, T_p, as a function of silicon content in Al6061 alloy for a constant heating rate (5 °C/min)

The results of the heating cycle show that the enthalpy, for the first detectable endothermal effect at around 833 °K, increased when Si content was increased from 2.5 to 10 wt%. It was proposed that the first peak is due to the localized melting, probably a binary eutectic, with the formation of a melt rich in Si in the presence of the α-solid solution and the compounds Al_2Si. In this situation, the liquid phase acts to shield the particle surface at temperatures over 866 °K and prevents the formation of AlN. This explains the absence of an exothermic peak attributed to AlN formation in the Al6061 alloys with Si addition. The second detectable thermal effect is a high temperature endothermic peak occurring around 911, 892, and 888 °K, for the alloy containing 2.5, 5.0, and 10.0 wt% Si, respectively. These peaks refer to a phase transition with the reaction enthalpy of 75, 54, and 72 mV s/mg. From these results, it can be concluded that the second peak is due to the melting of the binary eutectic. These results have shown that the value of enthalpy for the second endothermic peak was decreased when the content of Si was increased (Table 4).

Peak temperature

In order to investigate the influence of Si on the peak temperature of the endothermic peak (T_p) (as observed during melting of the alloys), the peak temperature is plotted against Si content in Fig. 6. An increase of Si content results in an increase of dissolution peak temperature which means that the dissolution rate is faster by Si addition. This plot approximates the liquidus curve in the Al–Si phase diagram, indicating the expected decrease in melting with increased alloying. However, the endotherm associated with the nitrogen reaction is overlaid with the melting reaction, so the peak height is reduced by the simultaneous nitridation reaction over this same temperature range.

Effect of SiC content

Figure 2 and Table 5 show DSC test results of Al alloys with SiC. We have noticed that addition of SiC has no influence on changing the position of the onset and peak temperatures in DSC test based on the comparison of IDs 1 (AlAl6061) and 5 (AlAl6061 + 10SiC) and IDs 4 (AlAl6061 + 10Si) and 6 (AlAl6061 + 10Si + 10SiC). These dispersed particles are stable at the processing temperature which can possibly change grain growth and crystallization characteristics.

Conclusions

DSC investigation was performed to understand the influence of Si, SiC and the atmosphere on the heat flow and micro-structural changes. From the results obtained in this study it can be concluded that:

- Nitrogen reactions with aluminum and the formation of aluminum nitride gives an endothermic peak in the

Table 5 DSC parameter of the Al6061 alloy containing various amounts of Si and SiC

ID	Composition	Onset temperature/K		Peak temperature/K		Enthalpy/mV s mg^{-1}	
		Onset I	Onset II	Peak I	Peak II	Peak I	Peak II
1	AlAl6061	866	–	928	–	75	–
2	AlAl6061 + 2.5Si	823	851	833	911	9.2	75
3	AlAl6061 + 5Si	820	858	845	892	14.9	54
4	AlAl6061 + 10Si	820	–	852	–	70	72
5	AlAl6061 + 10SiC	867	–	927	–	54	–
6	AlAl6061 + 10Si + 10SiC	819	–	853	–	72	–
7	Al6061 (Ar)	912	–	928	–	61	–
8	AlAl6061 + 10SiC (Ar)	912	–	928	–	54	–
9	AlAl6061 + 10Si + 10SiC (Ar)	834	–	853	–	72	–

same temperature range as where reactions occur between aluminum and silicon. Heating in argon avoids the nitridation reaction.

- Al6061 alloys containing Si (2.5–10 wt%) show a first endothermic peak occurring in the temperature range of 823–848 °K due to the localized melting, probably a binary eutectic, producing a high silicon melt in the presence of the intermetallic compound Al_2Si. Increasing of the Si content in the alloy increases the value of enthalpy for the first peak. The second endothermal peak occurs due to the local melting of the binary eutectic. The value of enthalpy for the second endothermic peak decreased when the content of Si is increased. During cooling, the coarsening of the silicon particles causes the peaks to shift toward low temperature values with an increase in Si content.
- The heat produced by dissolution of silicon has been determined from the experiments with Al6061 alloys, to be in the range of 54–75 mV s/mg with a decrease in silicon content. The precipitation of silicon starts earlier in Al–2.5Si than in Al–5Si which is, in turn, earlier than Al–10Si alloys because of a larger driving force due to a larger silicon supersaturation.
- DSC analysis of Al6061 alloys containing different amounts of Si content shifts the temperature of the first endothermal peaks. The enthalpy for the first endothermal peak was decreased with a decrease in Si content, while the second endothermal peak enthalpy decreased with increasing Si content in the alloy. We investigated that SiC addition has no influence on the enthalpy of the systems.

References

1. Manna A, Bhattacharayya. A study on machinability of Al/SiC-MMC. J Mater Process Technol. 2003;140:711–6.
2. Tanaka H, Inomata H, Hara K, Hasegawa H. Normal sintering of aluminum-doped β-silicon carbide. J Mater Sci Lett. 1985;4:315–7.
3. Lin BW, Imai M, Yano T, Iseki T. Hot-pressing of β-silicon carbide powder with aluminum-boron-carbon additives. J Am Ceram Soc. 1986;69:C67–8.
4. Padture NP. In situ-toughened silicon carbide. J Am Ceram Soc. 1994;77:519–23.
5. Papazian JM. Effects of silicon carbide whiskers and particles on precipitation in aluminum matrix composites. Metall Trans. 1988;19A:2945–53.
6. Bermudez VM. Auger and electron energy-loss study of the aluminum/silicon carbide interface. Appl Phys Lett. 1983;42:70–2.
7. Porte L. Photoemission spectroscopy study of the aluminum/silicon carbide interface. J Appl Phys. 1986;60:635–8.
8. Kannikeswaran K, Lin RY. Trace element effects on aluminum-silicon carbide interfaces. J Met. 1987;39:17–9.
9. Arsenault RJ. The strengthening of aluminum alloy 6061 by fiber and platelet silicon carbide. Mater Sci Eng. 1984;64:171–81.
10. Rack HJ, Krenzer RW. Thermomechanical treatment of high purity 6061 aluminum. Metall Trans. 1977;8A:335–46.
11. Inem B. Crystallography of the second phase/SiC particles interface, nucleation of the second phase at β-SiC and its effect on interfacial bonding, elastic properties and ductility of magnesium matrix composites. J Mater Sci. 1995;30:5763–9.
12. Smith JA, Limthongkul L, Sass L. Microstructures and mechanical properties of Ni-MgO composites formed by displacement and partial reduction reactions. Acta Mater. 1997;45:4241–50.
13. Lee JC, Kim GH, Lee HI. Characterization of interfacial reaction in (Al_2O_3)p/6061 aluminum alloy composite. Mater Sci Technol. 1997;13:182–6.
14. Kondoh K, Kimura A, Watanable R. Effect of Mg on sintering phenomenon of aluminum alloy powder particle. Powder Metall. 2001;44:161–4.
15. Schaffer GB, Hall BJ, Bonner SJ, Huo SH, Secombe TB. The effect of the atmosphere and the role of pore filling on the sintering of aluminium. Acta Mater. 2005;54:131–8.
16. Martin JM, Castro FJ. Liquid phase sintering of P/M aluminium alloys: effect of processing conditions. J Mater Process Technol. 2003;814:143–4.
17. Schaffer GB, Hall BJ. The influence of the atmosphere on the sintering of aluminum. Metall Mater Trans. 2002;A33:3279–84.
18. Jha JA, Prasad SV, Upadhyaya GS. Effect of sintering atmosphere and alumina addition on properties of 6061 aluminum P/M alloy. J Powder Metall Int. 1989;20:18–20.
19. Fan T, Zhang D, Shi Z, Wu R, Shibayangai T, Naka M, et al. The effect of Si upon the interfacial reaction characteristics in SiCp/Al-Si system composites during multiple-remelting. J Mater Sci. 1999;34:5175–80.